
Study of autonomous conservative oscillator using an improved perturbation method

C. F. Sagar Zephania · Tapas Sil

Received: date / Accepted: date

Abstract In a recent article [1], Aboodh transform based homotopy perturbation method (*ATHPM*) has been found to produce approximate analytical solutions in a simple way but with better accuracy in comparison to those obtained from some of the established approximation methods [2,3] for some physically relevant anharmonic oscillators such as, autonomous conservative oscillator (ACO). In this article, expansion of frequency (ω) and an auxiliary parameter (h) are introduced in the framework of homotopy perturbation method (HPM) to improve the accuracy by retaining its simplicity. Laplace transform is used to make the calculation simpler. This improved HPM (*LTHPMh*) is simple but provides highly accurate results for ACO in comparison to those from *ATHPM*.

PACS 31.15.xp, · 43.40.Ga

1 Introduction

Autonomous conservative oscillator is an anharmonic oscillator with strong non-linearity. Anharmonic oscillators are the systems generalizing the simple linear harmonic oscillator and are widely used for modeling many physical phenomena [4,5,6,7,8,9]. Finding solutions to the problems involving anharmonicity are difficult and most of them are not exactly solvable. Although, solving the anharmonic oscillator problems numerically are sometimes easy, one desires to get the analytical solutions of such problems as they carry more information and hence give a better insight about the system. There are many techniques for solving nonlinear oscillator problems such as the harmonic balance method [10], weighted linearization method [11], perturbation procedure for limit cycle analysis [12], modified Lindstedt-Poincare method [13], Adomian decomposition method [14] and so on.

Department of Physics, Indian Institute of Information Technology Design and Manufacturing Kancheepuram, Chennai-600127, Tamil Nadu, India

Department of Physics, Indian Institute of Information Technology Design and Manufacturing Kancheepuram, Chennai-600127, Tamil Nadu, India
E-mail: tapassil@iiitdm.ac.in

Most of these methods are not only somewhat plagued with the complexity of calculation but also fails to handle problems with strong nonlinearity properly. Recently, a few techniques are proposed to obtain an analytical solution to the dynamical systems with nonlinearity which are found to yield very good results without any higher-order approximation [15, 16]. One still strives for finding a technique which is simple but yields accurate solutions to the governing equation of the anharmonic oscillators.

Liao [17, 18] proposed an analytical method, in 1992, known as the homotopy analysis method (HAM) which introduces an embedding parameter to construct a homotopy of the given system and then analyzes it by means of the Taylor formula. Subsequently, by means of the property of homotopy, one can transform a nonlinear problem into an infinite number of linear subproblems, irrespective of the fact that the nonlinear problem contains small parameters or not. Therefore, unlike the perturbation method, this method does not depend on the values (smallness) of the perturbing parameter. Moreover, HAM provides a way to ensure the convergence of solution series introducing an auxiliary parameter. On the other hand, J. H. He developed the homotopy perturbation method (HPM) for solving nonlinear problems with given initial or boundary condition [19, 20]. HPM is found to be very efficient in solving several problems with strong non-linearity in classical [19, 20, 21] as well as quantum mechanical domain [22]. In this method, the solution is given in an infinite series usually converging to an accurate solution [23, 24]. In fact, HPM is a special case of HAM [25, 26] providing simpler calculation in solving problems. Hence, sometimes it compromises with the accuracy. We have considered an expansion of frequency (ω) in the framework of HPM [22] to improve the accuracy of calculation and also adopted an auxiliary parameter (h) [18] to control the convergence. Laplace transform (LT) has been applied for making the calculation of solving differential equations further simple [27]. The Laplace transform based HPM with h ($LTHPMh$) gives a simple way to achieve very high accuracy in solving nonlinear equations.

$LTHPMh$ is used to get the displacement (x) and ω for strongly nonlinear ACO. We compare $LTHPMh$ results to those obtained from $ATHPM$ and Hamiltonian approach technique (HT) [28] where the results from numerical calculations ($RK4$) are considered as the benchmark for checking the accuracy.

This paper is organized as follows. In section 2, we demonstrate briefly the formulation of $LTHPMh$. Application of $LTHPMh$ for studying an autonomous conservative oscillator has been shown in section 3. Finally, we provide a brief discussion and conclusions in section 4.

2 Formalism

Let us consider a nonlinear inhomogeneous differential equation,

$$G[\ddot{x}, \dot{x}, x, g] = 0, \quad (1)$$

subjected to the initial conditions,

$$\begin{aligned} x(0) &= a, \\ \dot{x}(0) &= 0, \end{aligned} \quad (2)$$

where, \dot{x} denote the differentiation of x with respect to the time (t), G is the second order nonlinear differential operator and g is the inhomogeneous term. We can construct a homotopy of equation (1) as given below,

$$(1-p)U[x-x_g] + hpG[\ddot{x}, \dot{x}, x, g] = 0, \quad (3)$$

where,

$$U[x] = \ddot{x} + \omega^2 x. \quad (4)$$

Here, $p \in [0,1]$ is an embedding parameter and $x_g = a \cos \omega t$ is the initial approximation of $x(t)$ satisfying the conditions in equation (2) with frequency ω . For $p = 0$, equation (3) is exactly solvable, whereas $p = 1$ corresponds to the nonlinear problem for which we are trying to find out the solution. The convergence control parameter h is incorporated in equation (3). Using the transformation, $\tau = \omega t = \frac{t}{\sqrt{\Lambda}}$, in equation (3), one can write,

$$(1-p)(x'' + x - x_g'' - x_g) + phM[x'', x', x, g, \Lambda] = 0, \quad (5)$$

with the initial conditions,

$$\begin{aligned} x(\tau = 0) &= a, \\ x'(\tau = 0) &= 0, \end{aligned} \quad (6)$$

where, the prime denotes the differentiation with respect to τ and M stands for the second order nonlinear differential operator after the transformation is taken. Applying, LT on both sides of the equation (5) and using the derivative property, $L[x^n(\tau)] = s^n L[x(\tau)] - s^{n-1}x(0) - s^{n-2}x'(0) - \dots - x^{n-1}(0)$, of the LT [27] and then applying initial conditions, we get,

$$(1-p)L[x-x_g] = \frac{-ph}{s^2+1}L\left[M[x'', x', x, g, \Lambda]\right]. \quad (7)$$

Using inverse LT on both sides of equation (7), we get,

$$x = x_g + p(x - x_g) - L^{-1}\left\{\frac{ph}{s^2+1}L[M[x'', x', x, g, \Lambda]]\right\}. \quad (8)$$

Using HPM, we can expand x and Λ in power series of p as follows,

$$x = \sum_{n=0}^{\infty} x_n p^n = x_0 + x_1 p + x_2 p^2 + \dots, \quad (9)$$

$$\Lambda = \sum_{n=0}^{\infty} \Lambda_n p^n = \Lambda_0 + \Lambda_1 p + \Lambda_2 p^2 + \dots \quad (10)$$

Substituting equations (9) and (10) in equation (8) and equating the coefficients p^0, p^1, p^2, \dots , we get the contributions from higher order approximations to the displacement, such as,

$$p^0: \quad x_0(\tau) = x_g, \quad (11)$$

$$p^1: \quad x_1(\tau) = L^{-1}\left\{\frac{-h}{s^2+1}\left(L[f_0[x_0'', x_0', x_0, \Lambda_0]]\right)\right\}, \quad (12)$$

$$p^2: \quad x_2(\tau) = x_1(\tau) - L^{-1}\left\{\frac{h}{s^2+1}L[f_1[x_0'', x_0', x_0, x_1'', x_1', x_1, \Lambda_0, \Lambda_1]]\right\}, \quad (13)$$

where, the f_0 and f_1 are functionals. The approximate solution is obtained putting $\tau = \omega t$ and $p = 1$,

$$x(t) = x_0(t) + x_1(t) + x_2(t) + \dots, \quad (14)$$

$$\omega = (A_0 + A_1 + A_2 + \dots)^{-1/2}. \quad (15)$$

We calculate the average value of square residual of the differential equation for choosing the proper value of h [18],

$$E_m(h) = \frac{1}{2\pi} \int_0^{2\pi} [\Delta_m(\tau, h)]^2 d\tau, \quad (16)$$

where,

$$\Delta_m(\tau, h) = N[\tilde{x}''', \tilde{x}', \tilde{x}, g, \tilde{A}], \quad (17)$$

is the residual of the governing equation, and

$$\tilde{x} = \sum_{n=0}^m x_n(\tau), \quad \tilde{A} = \sum_{n=0}^m A_n. \quad (18)$$

In equation (18), $\tilde{x}(\tau)$ and \tilde{A} , corresponds to the approximation up to m^{th} order of $x(\tau)$ and A , respectively. For converged solution, $E_m(h)$ should be minimum. Therefore,

$$\frac{dE_m(h)}{dh} = 0. \quad (19)$$

The parameter h can be chosen by evaluating the minimum value of the averaged square residual, $E_m(h)$, from equation (19). For the purpose of computational efficiency, equation (16) is discretized as,

$$E_m(h) = \frac{1}{q+1} \sum_{k=0}^q [\Delta_m(\tau_k, h_0)]^2; \quad \tau_k = \frac{2k\pi}{q}, \quad (20)$$

where q is an integer. The value of q is taken as 50 for the calculations presented in the article.

3 Applications

The equation of motion of the autonomous conservative oscillator (ACO) is given by,

$$\ddot{x}(1 + \epsilon x^2 + \alpha x^4) + \lambda x + \epsilon x \dot{x}^2 + 2\alpha x^3 \dot{x}^2 + \beta x^3 + \gamma x^5 = 0, \quad (21)$$

with initial conditions, $x(0) = a$ and $\dot{x}(0) = 0$. The parameter λ is an integer which may take values from $-1, 0$ and 1 whereas ϵ, α, β and γ are positive parameters. In this article, $\lambda = 1$ is considered for computation of displacements and frequencies of ACO for different values of the other parameters. Homotopy of equation (21) is constructed as follows,

$$(1-p)U[x - x_g] + hp(\ddot{x}(1 + \epsilon x^2 + \alpha x^4) + \lambda x + \epsilon x \dot{x}^2 + 2\alpha x^3 \dot{x}^2 + \beta x^3 + \gamma x^5) = 0. \quad (22)$$

Introducing the transformation, $\tau = \frac{t}{\sqrt{A}}$ in equation (22), we get,

$$(1-p)[x'' + x - x_g'' - x_g] + ph(x''(1 + \epsilon x^2 + \alpha x^4) + \Lambda \lambda x + \epsilon x x'^2 + 2\alpha x^3 x'^2 + \Lambda \beta x^3 + \Lambda \gamma x^5) = 0, \quad (23)$$

where prime denotes the differentiation with respect to τ . Using LT on both sides of equation (23) and using the derivative property of the LT [27] and initial conditions followed by inverse LT, we may write,

$$x(\tau) = x_g + p(x - x_g) - hL^{-1} \left\{ \frac{1}{s^2 + 1} pL [x''(1 + \epsilon x^2 + \alpha x^4) + \Lambda \lambda x + \epsilon x x'^2 + 2\alpha x^3 x'^2 + \Lambda \beta x^3 + \Lambda \gamma x^5] \right\}. \quad (24)$$

Substituting equations (9) and (10) in (24) and equating the coefficient of $p^0, p^1, p^2..$ etc., we get,

$$p^0 : \quad x_0(\tau) = x_g, \quad (25)$$

$$p^1 : \quad x_1(\tau) = -hL^{-1} \left\{ \frac{1}{s^2 + 1} L [x_0''(1 + \epsilon x_0^2 + \alpha x_0^4) + \Lambda_0 \lambda x_0 + \epsilon x_0 x_0'^2 + 2\alpha x_0^3 x_0'^2 + \Lambda_0 \beta x_0^3 + \Lambda_0 \gamma x_0^5] \right\}, \quad (26)$$

$$p^2 : \quad x_2(\tau) = x_1 - hL^{-1} \left\{ \frac{1}{s^2 + 1} L \left[\gamma \Lambda_1 x_0^5 + x_1 \{ \lambda \Lambda_0 + \epsilon x_0'^2 \} + x_0^3 \{ \beta \Lambda_1 + 4\alpha x_0' x_1' + 4\alpha x_1 x_0'' \} + x_0 \{ \lambda \Lambda_1 + 2\epsilon x_0' x_1' + 2\epsilon x_1 x_0'' \} + x_1'' + x_0^4 \{ 5\gamma \Lambda_0 x_1 + \alpha x_1'' \} + \{ \epsilon x_1'' + 3x_1 (\beta \Lambda_0 + 2\alpha x_0'^2) \} x_0^2 \right] \right\}, \quad (27)$$

Using the properties of LT followed by inverse LT in equation (26), we get,

$$x_1(\tau) = \frac{h}{16} [8a + 4\epsilon a^3 + 3\alpha a^5 - \Lambda_0(8a\lambda + 6\beta a^3 + 5\gamma a^5)] \tau \sin \tau + \frac{h}{128} [8\epsilon a^3 + 7\alpha a^5 - 4\Lambda_0 \beta a^3 - 5\gamma \Lambda_0 a^5] (\cos \tau - \cos 3\tau) + \frac{h a^5}{384} [3\alpha - \gamma \Lambda_0] (\cos \tau - \cos 5\tau) \quad (28)$$

The coefficient of $\tau \sin \tau$ in equation (28) needs to be equal to zero for avoiding the secular term, i.e.,

$$8a + 4\epsilon a^3 + 3\alpha a^5 - \Lambda_0(8a\lambda + 6\beta a^3 + 5\gamma a^5) = 0, \quad (29)$$

which gives Λ_0 as,

$$\Lambda_0 = \frac{8 + 3a^4 \alpha + 4a^2 \epsilon}{8\lambda + 5a^4 \gamma + 6a^2 \beta}. \quad (30)$$

Therefore, the frequency from the zeroth order approximation is,

$$\omega_0 = \sqrt{\frac{8\lambda + 5a^4 \gamma + 6a^2 \beta}{8 + 3a^4 \alpha + 4a^2 \epsilon}}, \quad (31)$$

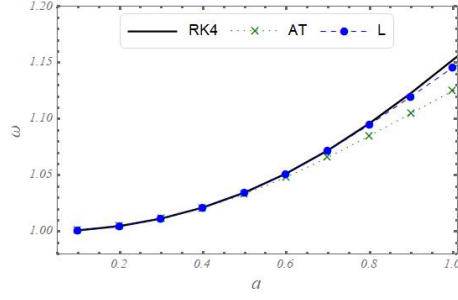


Fig. 1 The frequency (ω) of ACO obtained from ATHPM and LTHPMh are compared with those extracted from *RK4* results for different values of a with $OP = 1.0$

which is same as the frequency from the first order approximation in ATHPM [1] and HT [28]. The remaining part of $x_1(\tau)$ in equation (28) gives the first order approximation of x ,

$$x_1(\tau) = \frac{h}{128} [8\epsilon a^3 + 7\alpha a^5 - 4\Lambda_0 \beta a^3 - 5\gamma \Lambda_0 a^5] (\cos \tau - \cos 3\tau) + \frac{ha^5}{384} [3\alpha - \gamma \Lambda_0] \times (\cos \tau - \cos 5\tau). \quad (32)$$

Similarly, the coefficient of p^2 will also have a secular term and must be zero to have a physical solution which gives the first order correction to Λ , as given below,

$$\Lambda_1 = \frac{a^2 h}{192(6a^2 \beta + 5a^4 \gamma + 8\lambda)} [96a^2 \alpha - 15a^6 \alpha^2 + 96\epsilon - 12a^4 \alpha \epsilon - \Lambda_0(48\beta + 64a^2 \gamma + 138a^4 \alpha \beta + 150a^6 \alpha \gamma + 144a^2 \beta \epsilon + 156a^4 \gamma \epsilon + 96a^2 \alpha \lambda + 96\epsilon \lambda) + \Lambda_0^2(72a^2 \beta^2 + 174a^4 \beta \gamma + 105a^6 \gamma^2 + 48\beta \lambda + 64a^2 \gamma \lambda)]. \quad (33)$$

Therefore, considering first order correction to Λ , the frequency can be written as,

$$\omega = (\Lambda_0 + \Lambda_1)^{-1/2}. \quad (34)$$

The displacement of ACO, considering of the term upto first order is obtained as,

$$x_L(t) = a \cos \omega t + \frac{h}{128} [8\epsilon a^3 + 7\alpha a^5 - 4\Lambda_0 \beta a^3 - 5\gamma \Lambda_0 a^5] (\cos \omega t - \cos 3\omega t) + \frac{ha^5}{384} [3\alpha - \gamma \Lambda_0] (\cos \omega t - \cos 5\omega t), \quad (35)$$

where, the frequency ω is given in equation (34).

We display the calculated values of frequency (ω) as a function of amplitude (a) with $OP = 1$ using *ATHPM* (*HT*), *LTHPMh* and *RK4* in figure 1. Here, OP stands for the ‘‘other parameters’’ given in equation (21), *i.e.*, $OP = \alpha = \beta = \epsilon = \gamma$. It is seen from the figure that all approximate methods give same values as *RK4* at the lower amplitude for example, $\omega_{APPROX} = 1.00126$ at $a = 0.1$. At a larger amplitude, *LTHPMh* frequency remain very close to those obtained from *RK4* whereas *ATHPM* underestimates the ω . The percentage error in ω are 2.385 and 0.584 for *ATHPM* and *LTHPMh*, respectively, for $a = 1$ which reduce to 0.167 if the second order term in *LTHPMh* is considered.

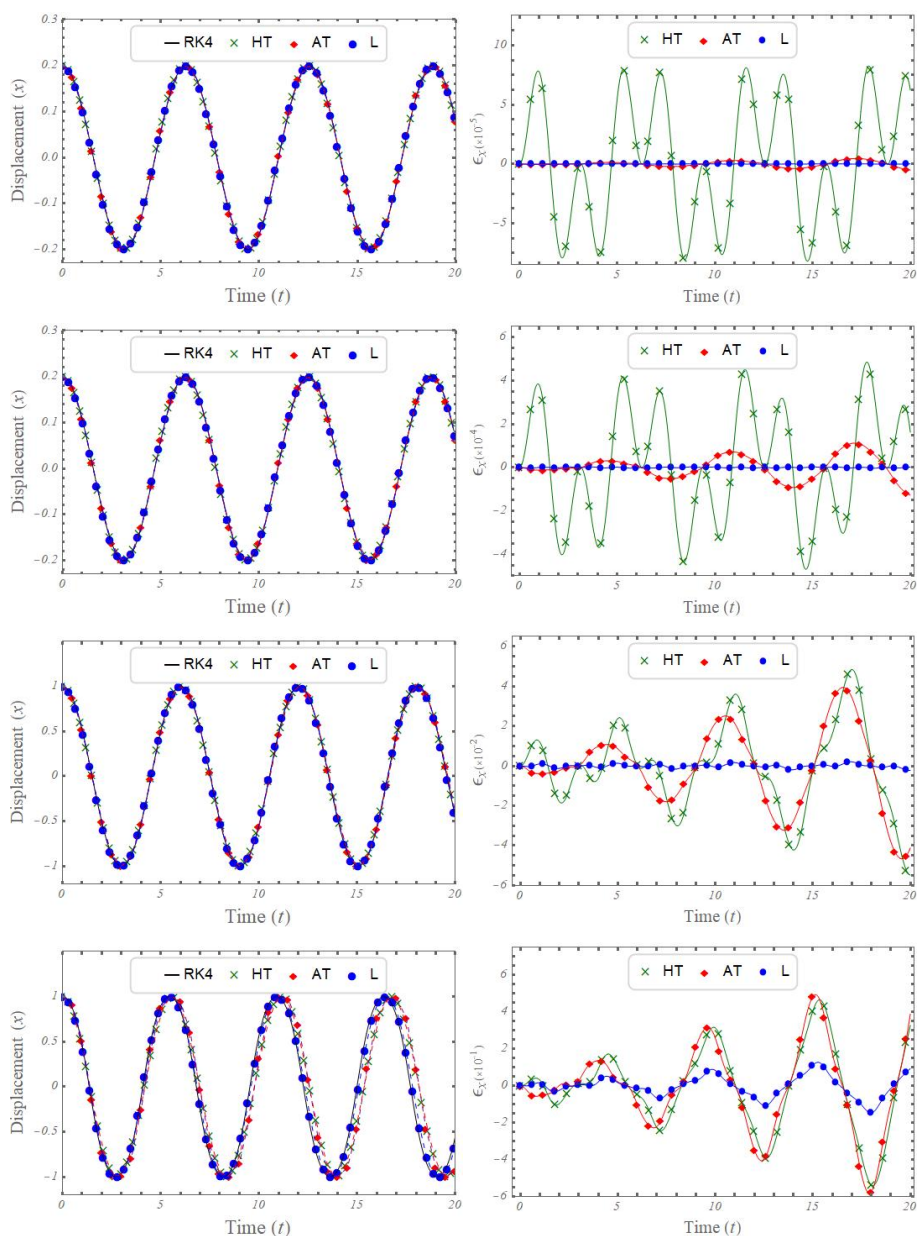


Fig. 2 Plot of variation of displacements x_{RK4} (black solid line), x_{HT} (green cross), x_{AT} (red diamond), and x_L (blue circle) with time (t) are shown in the four panels of the left column for four parameter sets A, B, C, and D starting from the top panel to bottom panel, respectively. Absolute errors in the approximate solutions (HT , $ATHPM$ and $LTHPMh$) with respect to $RK4$ for the same parameter sets are displayed in the right column.

Table 1 Values of h , rms error of approximate x with respect to x_{RK4} for different sets of parameters. Here, $u(-n)$ indicates $u \times 10^{-n}$.

a	OP	h	$\epsilon_{x_{HT}}^{rms}$	$\epsilon_{x_{AT}}^{rms}$	$\epsilon_{x_L}^{rms}$
0.2	0.2	0.996672	5.1200(-05)	2.1452(-06)	6.0990(-08)
0.2	0.8	0.986653	2.0514(-04)	3.3845(-05)	9.4916(-07)
0.2	1.0	0.983304	2.5725(-04)	5.2641(-05)	1.4724(-06)
0.8	0.2	0.903987	6.1287(-03)	4.7546(-03)	1.2546(-04)
0.8	0.8	0.667982	5.6830(-02)	5.4939(-02)	4.8592(-03)
0.8	1.0	0.607391	7.7976(-02)	7.6473(-02)	8.9997(-03)
1.0	0.2	0.818679	2.1314(-02)	1.9669(-02)	8.0067(-04)
1.0	0.8	0.478981	1.6981(-01)	1.7129(-01)	3.4287(-02)
1.0	1.0	0.413602	2.2266(-01)	2.2853(-01)	5.6200(-02)

We plot the displacements obtained from HT (x_{HT} , green cross) [28], $ATHPM$ (x_{AT} , red diamond) [1] and $LTHPMh$ (x_L , blue circles) expressed in equation (35) respectively, with increasing t for four sets of parameters A ($a = 0.2, OP = 0.2$), B ($0.2, 1.0$), C ($1.0, 0.2$) and D ($1.0, 1.0$) in the left column of figure 2, and compared with the same obtained by numerical solution of equation (21) employing the fourth order Runge-Kutta ($RK4$) method ($x_{RK4}(t)$, black solid line). It is seen that for small values of the parameters, approximate displacements match well with x_{RK4} but a significant deviations for x_{AT} and x_{HT} from x_{RK4} are noticed for large values of force parameters. The deviation (error) of the approximate displacements with respect to its values calculated using $RK4$ ($\epsilon_{x_{APPROX}} = x_{RK4} - x_{APPROX}$), ϵ_{x_L} , $\epsilon_{x_{AT}}$ and $\epsilon_{x_{HT}}$ are displayed in the panels of right column of figure 2 for the same parameter sets as taken for calculating the graphs presented in the corresponding panels of the left column. All panels in the right column show that accuracy of $x_L(t)$ is much improved in comparison to $x_{AT}(t)$ and $x_{HT}(t)$ throughout the range of time considered here.

In order to get a clear idea about the performance of $LTHPMh$, we display in table 1, the root mean square deviations ($\epsilon_{x_{APPROX}}^{rms}$) of x_{APPROX} from x_{RK4} are presented in fourth, fifth and sixth columns, respectively. The root mean square deviation is defined as,

$$\epsilon_{x_{APPROX}}^{rms}(t) = \sqrt{\frac{1}{N} \sum_{i=1}^N [x_{RK4}(t_i) - x_{APPROX}(t_i)]^2}, \quad (36)$$

where N represent the maximum number of points considered. Values of h obtained from equation (19) which are used to calculate x_L for different values of ' a ' (first column) and ' OP ' (second column) are tabulated in the third column. It is seen that h is decreasing with the increase in the values of a and/or OP . It is noticed from the table that both $\epsilon_{x_{HT}}^{rms}$ and $\epsilon_{x_{AT}}^{rms}$ are order of magnitude higher in comparison to $\epsilon_{x_L}^{rms}$. Variations of rms errors in x obtained from HT (green cross), $ATHPM$ (red diamond) and $LTHPMh$ (blue circle) with a are presented in left panel of figure 3 for $OP = 0.8$. It displays that the all curves almost coincide with each other (approximately zero error) for a low amplitude. The curves corresponding to HT and $ATHPM$ start diverging rapidly together from $LTHPMh$ curves approximately at $a = 0.4$ and reach the value approximately 0.17 at $a = 1$ whereas the rms error of x_L is 0.035. Therefore, $LTHPMh$ is found to yield much improved results in comparison to those obtained from HT and $ATHPM$. Plot of

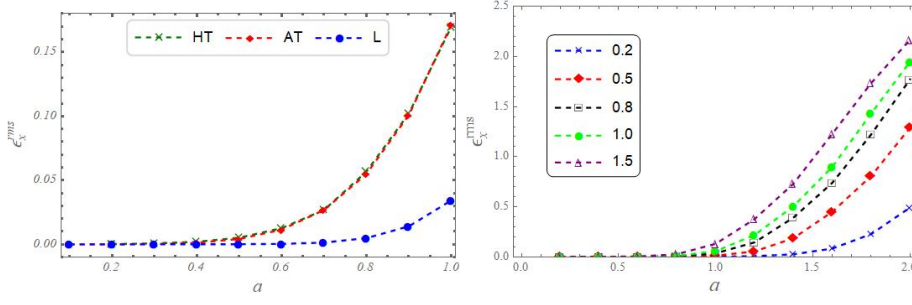


Fig. 3 Comparison of ϵ_x^{rms} (rms of ϵ_x) from *HT*, *ATHPM* with *LTHPMh* approximation with $OP = 0.8$. is displayed in the left panel. Plot of ϵ_x^{rms} with increasing a for different values of OP (right panel).

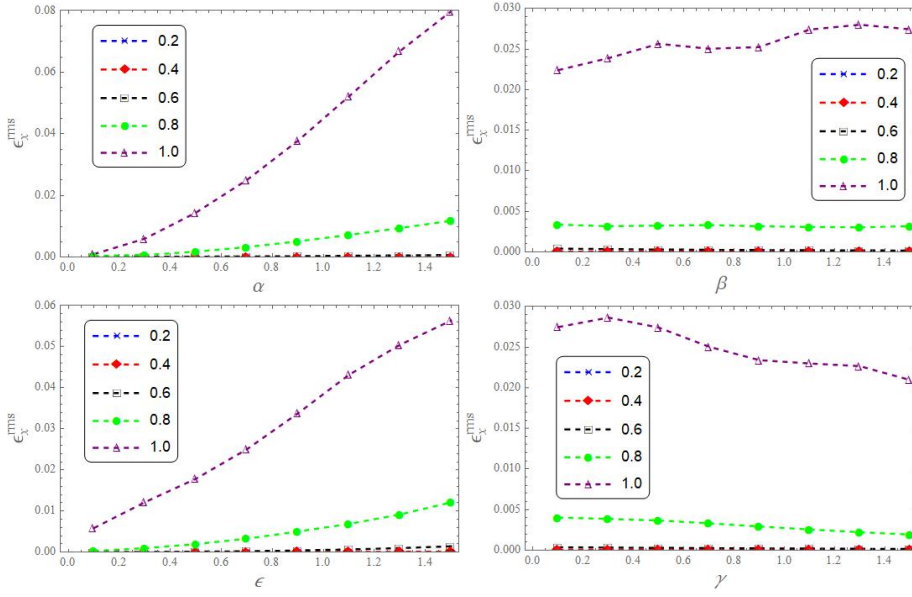


Fig. 4 Plot of ϵ_x^{rms} in *LTHPMh* displacement with respect to the α (left top), β (right top), ϵ (left bottom) and γ (right bottom) for different amplitudes a and $OP = 0.7$.

$\epsilon_{x_L}^{rms}$ with increasing amplitude for different values of OP starting from 0.2 to 1.5 are presented in the right panel of figure 3. The values of $\epsilon_{x_L}^{rms}$ remain very small up to $a = 1.0$ for all values of OP considered. The *rms* error starts increasing beyond $a = 1$ and reaches a high value at $a = 2.0$. It is noted that the rate of increase in $\epsilon_{x_L}^{rms}$ is more for a larger OP , i.e., stronger nonlinearity.

The changes in root mean square deviations of x obtained from *LTHPMh* with respect to the *RK4* values ($\epsilon_{x_L}^{rms}$) with increasing α (left top), β (right top), ϵ (left bottom) and γ (right bottom) for different amplitudes ($a = 0.2 - 1.0$ in steps of 0.2) taking $OP = 0.7$ are displayed in figure 4. It is observed from the left top panel that $\epsilon_{x_L}^{rms}$ are very small at very low amplitudes for the entire range of α considered. The *rms* errors increases for large values of α . The increase in $\epsilon_{x_L}^{rms}$ is more rapid for a larger value of a . The same is noted in the left bottom panel

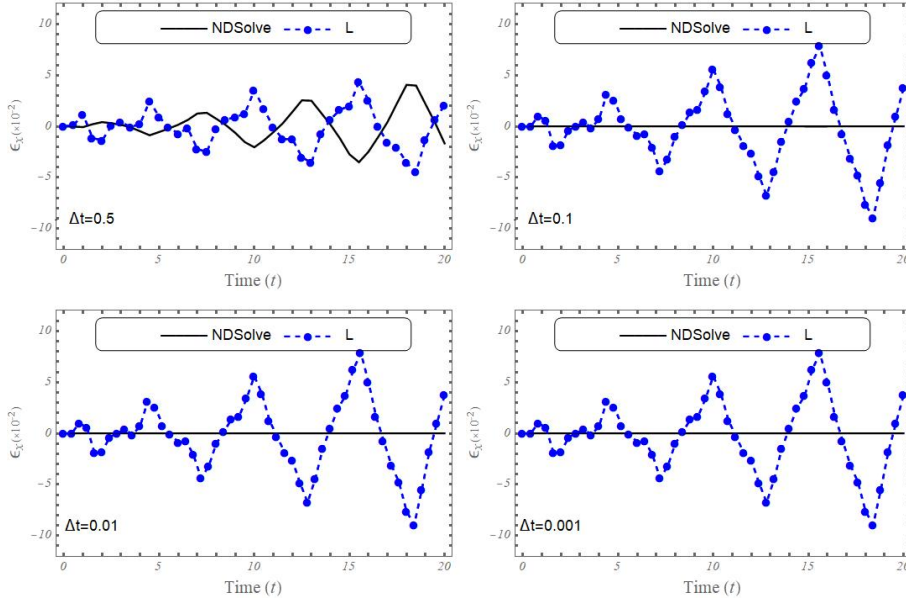


Fig. 5 Plot of error in displacement obtained from Mathematica function $NDSolve$ ($\epsilon_{x_{NDS}}$, black dotted line), and $LTHPMh$ (ϵ_{x_L} , blue circles) with respect to those calculated from $RK4$ versus time for different values of the mesh size (Δt) of time (t) for $a = 1.0$ and $OP = 0.8$.

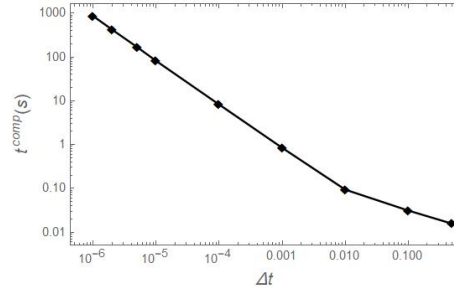


Fig. 6 Variation of computation time (t^{comp}) of $RK4$ calculation with step size in t for $a = 1$ and $OP = 0.8$

for ϵ . Right two panels show that $\epsilon_{x_L}^{rms}$ is not very sensitive to the variation of β and γ for a particular value of a . Though, the rms error increases for the increase in a for these two cases also.

Comparisons of the results obtained from $LTHPMh$, $ATHPM$ and HT are presented in previous figures and table considering the $RK4$ results as the reference. In order to check the reliability of $RK4$ results, we compute errors in displacement obtained from Mathematica function $NDSolve$ ($\epsilon_{x_{NDS}}$, black solid line) and $LTHPMh$ (ϵ_{x_L} , blue circles) with respect to those calculated from $RK4$. The variations of $\epsilon_{x_{NDS}}$ and ϵ_{x_L} with t are displayed in figure 5 for different mesh sizes ($\Delta t = 0.5, 0.1, 0.01$ and 0.001). It is observed that $\epsilon_{x_{NDS}}$ remains very close to zero throughout the span of time considered here for all values of Δt except 0.5.

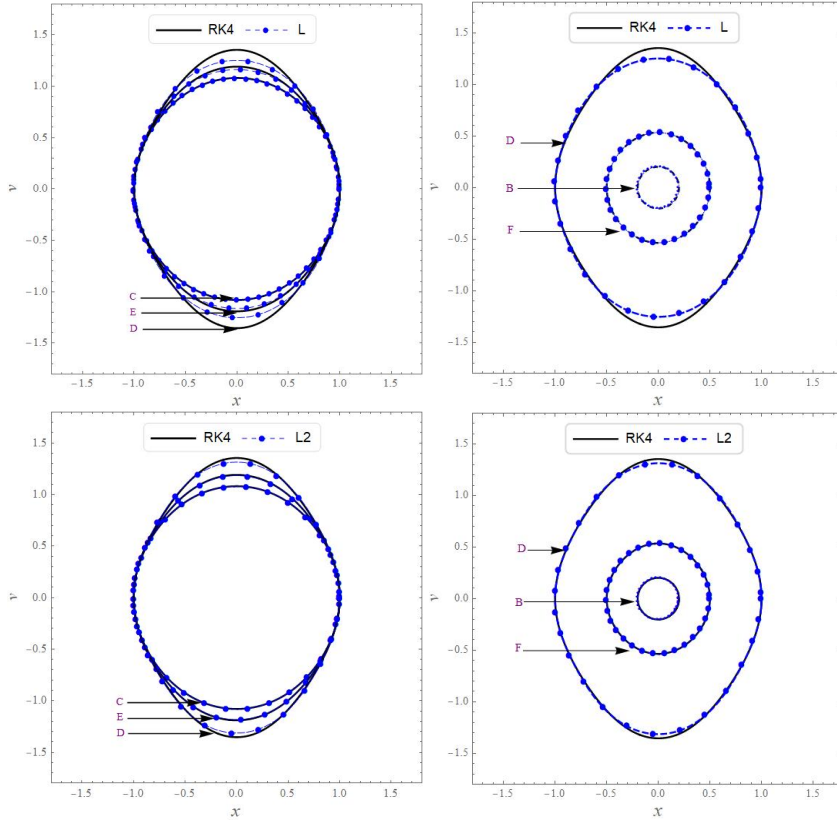


Fig. 7 Comparison of phase-space curve of the equation (21) obtained from LTHPMh and RK4. Top left panel compare the phase space curve for different OP for $a = 1.0$ whereas the top right panel compare phase curve for different a for $OP = 1.0$. Bottom two panels correspond to the second order LTHPMh ($L2$) calculations

Moreover, the profile of the ϵ_{x_L} curves and their maximum values are matching extremely well for all values of Δt except for 0.5. This ascertains the accuracy of the numerical solutions using RK4 if $\Delta t < 0.1$. Computation times (t^{comp}) for the solution of equation (21) with different Δt for $a = 1.0$ and $OP = 0.8$ is plotted in figure 6 (Mathematica is used in a computer with i7-7700, 3.60GHz and RAM=16GB). It is noted that t^{comp} starts increasing by an order of magnitude for the decrease in Δt by ten times from $\Delta t = 0.01$ onwards. Therefore, the mesh size, $\Delta t = 0.001$ is taken as the optimum one considering the convergence of solution and computation time. We have used this mesh size for all calculation presented in this article. It is noted that computational time for the calculation of x and ω using ATHPM is 7.35938s whereas the time increases to 13.5625s and 59.5313s for the first order and second order LTHPMh methods, respectively (for $a = 1$ and $OP = 1$).

Significant information about the motion and stability of a system can be extracted from phase portrait analysis. We plot the velocity, $v(= dx/dt)$ versus x obtained from LTHPMh and RK4 for the system described in equation (21).

In the top left panel of the figure 7, the phase-space curves are displayed for the parameter set C , D and $E(1.0,0.5)$ which shows that the approximate phase-space curve ($LTHPMh$) matches extremely well with $RK4$ curve for lower value of OP for amplitude $a = 1$ but for the higher values of the OP , i.e. when the nonlinearity becomes stronger, the $LTHPM$ phase curves deviate from the circular one and becomes more prolate keeping the center at origin $(0,0)$. In the top right panel of figure 7, phase-space curves are presented for different values of a with $OP = 1.0$ (parameter sets B , D and $F(0.5,1.0)$). Similar deviations of $LTHPMh$ curves from $RK4$ is observed for larger nonlinearity of the system due to the increased amplitudes. Both the panels of figure 7 confirms the periodic nature of the system with single stability point at the origin $(0,0)$ for the parameter sets considered here. The second order $LTHPMh$ phase curves ($L2$) are compared with $RK4$ results in bottom two panels and are found to exhibit similar trends but with better accuracy. Therefore, $LTHPMh$ can be reliably used for the phase-curves analysis.

4 Conclusion

An improved HPM ($LTHPMh$) is introduced to study oscillators with strong anharmonicity such as ACO. HPM is a simpler method than the HAM but in some cases it fails to yield accurate solution. In this article, a convergence parameter is introduced and the expansion of frequency term is also considered in the framework of HPM. Laplace transform is used to make the calculation easy. $LTHPMh$ is used to find the approximate analytical expression of displacement and frequency of oscillation for strongly nonlinear ACO and are compared to those obtained from HT , $ATHPM$ and numerical calculations ($RK4$). It is found that the new method gives the values of displacement and frequency with an accuracy at least one order of magnitude better than those of $ATHPM$ and HT for the parameter sets considered here. Comparison of rms deviations of displacement obtained from three aforementioned approximate methods are in corroborate with the conclusion that $LTHPM$ is a better approximate method. Results on rms deviations of displacements obtained from $LTHPMh$ quantify the effect of the strength of nonlinearity on the accuracy of the approximate result. Contributions of higher order terms are found to be nontrivial in calculating displacement and frequency of ACO, vibrating for long time and/or with large amplitude. $LTHPMh$ has been found to be trustworthy for analyzing phase portrait of a system. Computations of displacement and frequency for the cases considered in this article are very fast. It is to conclude that $LTHPMh$ is a blend of simplicity and delicacy. Hence, it can be used to study physical problems with strong nonlinearity, efficiently.

References

1. K. Manimegalai, C. F. S. Zephania, P. K. Bera, P. Bera, S. K. Das, T. Sil, Study of strongly nonlinear oscillators using the Aboodh transform and the homotopy perturbation method, Eup. Phys. J. Plus **134**, 462 (2019).
2. I Mehdipour, D D Ganji, and M Mozaffari, Application of the energy balance method to nonlinear vibrating equations, Curr. Appl. Phys. **10**, 104 (2010).

3. T A Nofal, G M Ismail, A A M Mady, and S Abdel-Khalek, Analytical and Approximate Solutions to the Free Vibration of Strongly Nonlinear Oscillators, *J. Electromagn. Anal. Appl.* **5(10)**, 388 (2013)
4. R A Bonham, L S Su, Use of HellmannFeynman and Hypervirial Theorems to Obtain Anharmonic VibrationRotation Expectation Values and Their Application to Gas Diffraction, *J. Chem. Phys.* **45**, 2827 (1966)
5. C M Bender, T T Wu, Anharmonic oscillator, *Phys. Rev.* **184**, 1231 (1969)
6. S -J Chang, Quantum fluctuations in a ϕ^4 field theory. I. Stability of the vacuum, *Phys. Rev. D* **12**, 1071 (1975)
7. C S Hsue, J L Chern, Two-step approach to one-dimensional anharmonic oscillators, *Phys. Rev. D* **29**, 643 (1984)
8. I S Ishmukhamedov, V S Melezhika, Tunneling of two bosonic atoms from a one-dimensional anharmonic trap, *Phys. Rev. A* **95**, 062701 (2017)
9. J C Prentice, B Monserrat, R J Needs, First-principles study of the dynamic Jahn-Teller distortion of the neutral vacancy in diamond, *Phys. Rev. B* **95**, 014108 (2017)
10. A H Nayfeh, D Mook, *Nonlinear oscillations*, (John Willey and Sons, New York, 1979)
11. V Agrwal, H Denman, Weighted linearization technique for period approximation in large amplitude non-linear oscillations, *J. Sound Vib.* **99**, 463 (1985)
12. S Chen, Y Cheung, S Lau, On perturbation procedure for limit cycle analysis, *Int. J. Nonlin. Mech.* **26**, 125 (1991)
13. Y Cheung, S Chen, S Lau, A modified Lindstedt-Poincar method for certain strongly non-linear oscillators, *Int. J. Nonlin. Mech.* **26**, 367 (1991)
14. G Adomian, A review of the decomposition method in applied mathematics, *J Math. Anal. Appl.* **135**, 501 (1988)
15. N.Herisanu, V. Marinca, G. Madescu, F. Dragan, Dynamic Response of a Permanent Magnet Synchronous Generator to a Wind Gust, *Energies* **12**, 915 (2019)
16. N. Anjum, J -H He, Laplace transform: Making the variational iteration method easier, *Appl. Math. Lett.* **92**, 134 (2019)
17. S J Liao, *The proposed homotopy analysis technique for the solution of nonlinear problems*, Ph. D. Thesis, Shanghai Jiao Tong University Shanghai (1992).
18. S. J. Liao, Notes on the homotopy analysis method: some definitions and theorems, *Commun. Nonlin. Sci Numer. Simulat.* **14**, 983 (2009)
19. J -H He, Homotopy perturbation technique, *Comput. Method Appl. M.* **178**, 257 (1999)
20. J -H He, A coupling method of a homotopy technique and a perturbation technique for non-linear problems, *Int. J. Nonlin. Mech.* **35**, 37 (2000)
21. J Biazar, M Eslami, A new homotopy perturbation method for solving systems of partial differential equations, *Comput. Math. Appl.* **62**, 225 (2011)
22. P Bera, T Sil, Homotopy perturbation method in quantum mechanical problems, *Appl. Math. Comput.* **219**, 3272 (2012)
23. A Yildirim, Retraction: Homotopy perturbation method to obtain exact special solutions with solitary patterns for Boussinesq-like B(m,n) equations with fully nonlinear dispersion, *J. Math. Phys.* **50**, 023510 (2009)
24. Z Ayati, J Biazar, On the convergence of Homotopy perturbation method, *J. Egypt. Math. Soc.* **23**, 424 (2015)
25. J.-H He, Comparison of homotopy perturbation method and homotopy analysis method, *Appl. Math. Comput* **156**, 527 (2004)
26. S. J. Liao, An analytic approach to solve multiple solutions of a strongly nonlinear problem, *Appl. Math. Comput.* **169**, 854 (2005)
27. G. B. Arfken, H. J. Weber, F. E. Harris, *Mathematical methods for physicists* (Academic Press, New Delhi, 2013)
28. M Hermann, M Saravi, H. E. Khah, Analytical study of nonlinear oscillatory systems using the Hamiltonian approach technique, *J Theor. Appl. Phys.* **8**, 133 (2014)